Chemometrics and Intelligent Laboratory Systems 185 (2019) 12–17

Contents lists available at ScienceDirect

Chemometrics and Intelligent Laboratory Systems

journal homepage: www.elsevier.com/locate/chemometrics

Image processing for three defects of topography images by SPM

Fan Xian-guang [a,b], Wang Xiao-dong [a], Chen Yu-xin [a], Wang Xin [a,b,*]

[a] Department of Instrumental and Electrical Engineering, Xiamen University, Xiamen, Fujian, 361005, PR China

[b] Fujian Key Laboratory of Universities and Colleges for Transducer Technology, Xiamen Key Laboratory of Optoelectronic Transducer Technology, Xiamen, Fujian, 361005, PR China

A R T I C L E I N F O

Keywords:
SPM
Topography image
Image processing
Background
Damage
Fringe

A B S T R A C T

Image processing plays an important role in the topography imaging by SPM. Due to the imperfect hardware and the environmental interference, the image defects can be easily found in the topography images. In order to deal with these defects, image processing technology is the most effective and convenient way, so image processing functions are integrated in most kinds of SPM software. In this study, we present image processing methods for three common defects of topography images: background, damage and fringe. According to the characteristics of the topography images and the defects, some algorithms are adopted in the proposed methods, such as B-spline, TV, Criminisi, Flourier transform and so on. The principles, processes and application scopes of the methods were described in detail, and the topography images with typical defects were selected to verify them. The processing results showed the feasibility of the methods, which offer an effective approach to acquire high-quality topography images in a fast, simple and cheap way.

1. Introduction

Scanning probe microscopy (SPM) has become a powerful imaging tool for submicron surface analysis and nanoscopic structures, which has applications in physics, materials science, chemistry, biology and nanotechnology [1–6]. Although SPM has proven its multi-functional abilities as 'the eyes and the fingers' of nanotechnology, the most relevant application of a SPM is still to acquire high-resolution topography images [7–9]. Hence, image processing is a central issue for any SPM software [10,11].

Nowadays, computers have played a central role in the development of SPM significantly improving the data acquisition, control, image processing, and data analysis. Hence, it is possible to introduce various algorithms for topography image processing. In this paper, we focus on three common defects of topography images which are often encountered in our experiments, and propose three processing methods. The defects to be processed are background, damage and fringe, as presented in Fig. 1.

Background is almost the most common problem of the topography images. There are two main reasons for background: mechanical precision and edge effect (Fig. 7, left and right). Theoretically, to acquire the true topographies of the samples, the scanning surface of probe and the scanning stage must be parallel. But it is too difficult or expensive to achieve this mechanical precision at the nanometer scale; edge effect causes the scanning probe to drop rapidly at the edge of the samples, especially for AFM due to the decrease of the atomic density at the edges. Although most software of SPMs have the background subtraction function, their background fitting algorithms can be easily over fitted when the samples have a relatively high step or a number of consecutive small steps. Once the over-fitting occurs, the chromatic aberration will appear near the step edges after subtracting the background, as shown in the left image of Fig. 1.

Image damage is usually caused by three main reasons [12,13], vibration interference, control delay and impurities on the sample surface. Vibration interference comes from the scanning stage or the external environment during the scanning (the first image in Fig. 9); control delay means the probe control system delay, which is usually caused by the large particles on the sample surface (the second image in Fig. 9); impurities often lead to large scale of damages (the second image in Figs. 2 and 8). Therefore, damages have multiple representations on the topography images, so it is difficult to deal with them by just one algorithm. In this paper, we introduce two algorithms according to the specific situation of different damages.

Noise is almost the most common phenomenon in instruments, as well as SPMs. Nowadays, in some well-equipped SPMs, the Gauss noise from the electron devices and the impulsive noise from the vibration of

* Corresponding author. Department of Instrumental and Electrical Engineering, Xiamen University, Xiamen, Fujian, 361005, PR China.
E-mail address: xinwang@xmu.edu.cn (W. Xin).

https://doi.org/10.1016/j.chemolab.2018.12.013
Received 7 August 2017; Received in revised form 17 December 2018; Accepted 24 December 2018
Available online 26 December 2018

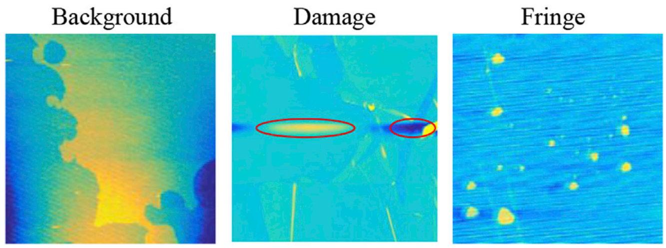

Fig. 1. Three common defects of topography images. Three kinds of defects are processed in this paper: 1. Background; 2. Damage; 3. Fringe.

scanning stage can be basically eliminated by reasonable circuit and anti-vibration design. However, to acquire high-quality images, Charge-coupled Devices (CCDs) with self-cooling function are very popular in the SPMs which bring the periodic noise due to the refrigeration motors. For example, the fringes of the right image in Fig. 1 are caused by the periodic noise. We haven't found the function to suppress the fringes in the commercial SPMs until now, so we propose an algorithm to deal with it.

2. Methods

2.1. Background subtraction with mask

Chromatic aberration of the topography images can be easily caused by subtracting the over-fitted background. The conventional method usually applied a quadric polynomial surface to fit the background of the image (Fig. S1). However, the step-region, which is a sudden change region, cannot be well recognized by polynomial, so an unexpected protuberance is appeared in the fitted background surface and cause the collapse after being subtracted.

In this paper, two improvements are made to the conventional method. Firstly, a mask is generated to cover the step-region from being fitted as background, so the step-region is actually a flat surface during fitting the background (Fig. 2). The mask is generated by two steps: edge detection and threshold. The edge gradient is mapped by edge detection operator from the raw image, and the mask is generated by threshold subsequently. Detailed information of the threshold step is presented in Fig. 3. The other improvement is adopting B-spline, instead of polynomial, to fit the background (Fig. S2). The advantage of B-spline [14] is its characteristics of low order and smooths, so B-spline algorithm is suitable for more kinds of complex background surface modeling. Although polynomial can be also used to model the complex surfaces by increasing order, the over-fit phenomenon can easily occurred. Equation S(1) is the background surface described by B-spline; Equation S(2) is the basic function of B-spline in x direction (y direction is similar), where tx is the preset B-spline knot vector; Equation S(3) is the optimal formula under least squares to calculate the optimal parameters $\mathbf{c}_{u,v}$ of Equation S(1).

2.2. Image inpainting by TV and criminisi algorithms

The main causes of image damages have been summarized last section. In this part, we sort out the types of damages: small/large scale and boundary/non-boundary damage (Fig. S3), for different types of damages, different algorithms should be applied. Two algorithms, Total Variation (TV) algorithm and Criminisi algorithm [15,16], are adopted to inpaint the boundary damage and the large scale damage respectively.

No matter TV or Criminisi algorithms, the damaged area should be marked artificially first. TV algorithm is a kind of algorithms based on structural information of the images. The main idea is to diffuse the information of the pixels outside the boundary of the inpainted/non-damaged area to the boundary continuously until the whole image is inpainted. So TV algorithm fixes the images in pixels and is suitable for inpainting the boundary damages, the principle and flow chart are shown in Fig. 4.

Criminisi algorithm is the other kind of algorithms based on texture information of the images. The main idea is to fill the damaged area by the best matching blocks in the undamaged area. So Criminisi algorithm fixes the images in blocks and is suitable for inpainting the large scale damages. A 3*3 block size is applied in this paper, and detailed principle of Criminisi algorithm is shown in Fig. 5.

2.3. Fringe-suppression by FT and notch filter

As mentioned before, the main reason for the fringes of topography images are periodic noise caused by the CCD refrigeration motor. Therefore, to suppress the fringes, the frequency of the noise source is located in the frequency domain first, and then the filter can be adopted. In the paper, 2D Fourier transform [17] is used to obtain the Fourier spectra of the raw topography image, and the edge detection (Sobel operator) is used to locate the frequency suppression points (frequency of

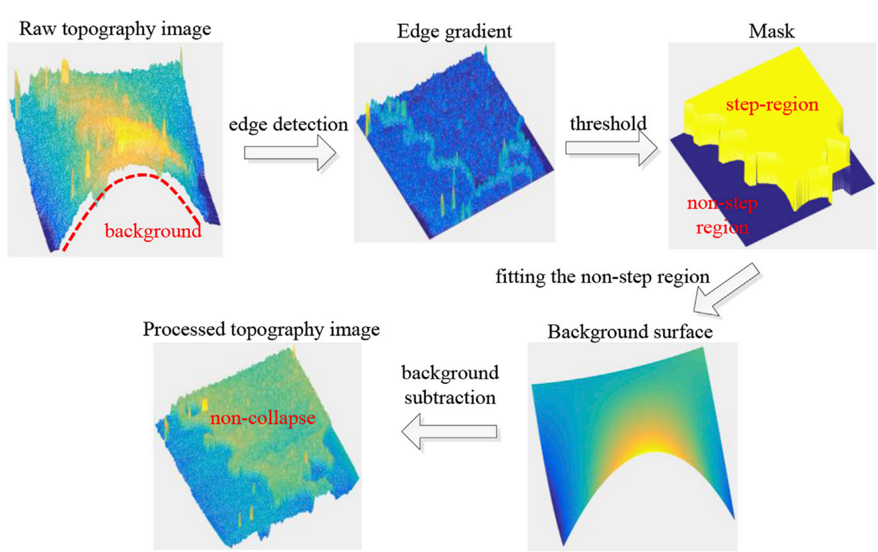

Fig. 2. Principle of the proposed method for background subtraction. The method can be divided into four steps: 1. Edge detection; 2. Threshold and generate the mask; 3. Background fitting; 4. Subtract the fitting surface from raw image.

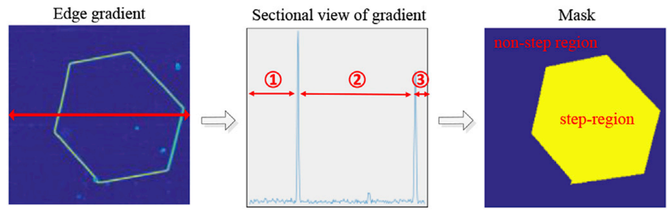

Fig. 3. Details of the threshold step in 2D view for background subtraction.

the periodic noise) which are the peak points of the edge gradient map. Here, the peak points are the local maxima of the edge gradient map in addition to the central area and the central cross lines. The notch filter can then be designed according to the frequency suppression points and applied to filter the periodic noise. At last, Fourier inversion is used, and the fringe suppressed image is obtained. The principle and flow chart are shown in Fig. 6, where the 'Fourier transform' in Fig. 6 is actually short for two-dimensional discrete Fourier transform. Equations S4 and S5 are the formulas of Fourier transform and inversion; Equation S(6) is the transfer function of Butterworth notch filter with two frequency suppression centers D_{k+} and D_{k-} (notch points, circle or ellipse).

3. Results and discussion

In this section, topography images of typical samples were chose to verify the proposed methods. The instrument is the NTEGRA Spectra from NT-MDT Company. All the topography images were obtained by its STM module under constant current mode with 400–600 pA tunneling current, 200–300 mV bias voltage, 0.8 Hz line scanning rate, 256*256 points and 500 nm*500 nm scanning range.

3.1. Background subtraction

To verify the proposed method, two typical samples were used in the experiments: gold nanoplate[18] and Au (111) single crystal[19]. As shown in Fig. 7, the gold nanoplate had a high step and the Au (111) single crystal had long and irregular step with significant background bending. Chromatic aberration can be observed in the raw images as well as the processed images by conventional method in 2D view. Obviously, the cause of chromatic aberration for conventional method was the collapse in 3D view due to the over-fit of the background surface. Owing to the mask of the proposed method, the step regions were well protected, so the collapse didn't happen and the step regions were clear without chromatic aberration.

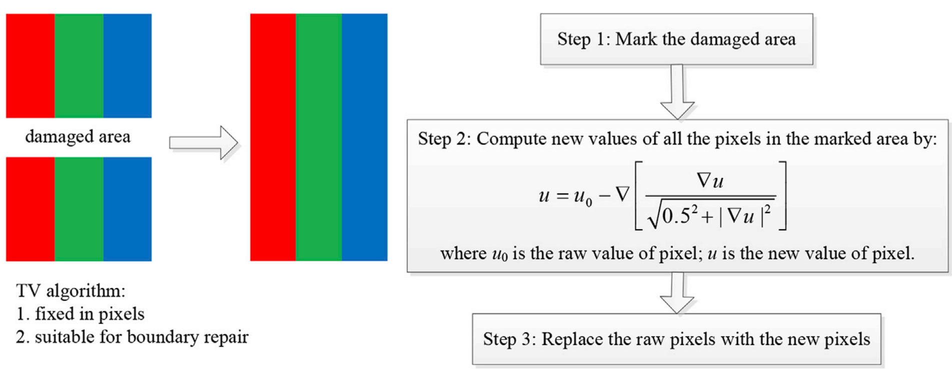

Fig. 4. Principle of TV algorithm for boundary inpainting. The main idea is computing the new value of each pixel in the damaged area based on its raw value and gradient.

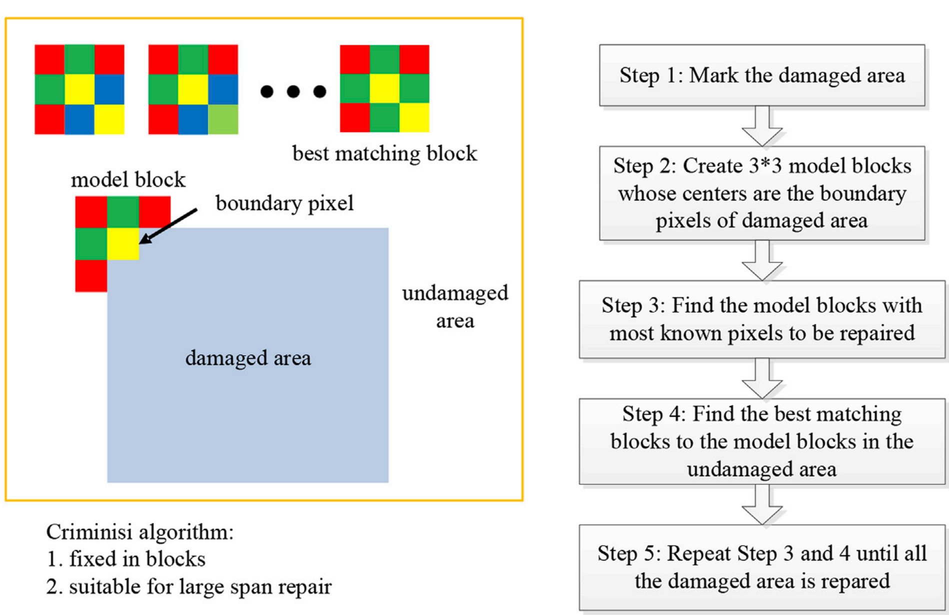

Fig. 5. Principle of Criminisi algorithm for large scale inpainting. The main idea is finding the best matching blocks from the undamaged area and filling them to the damaged area recurrently until all the damaged area is inpainted.

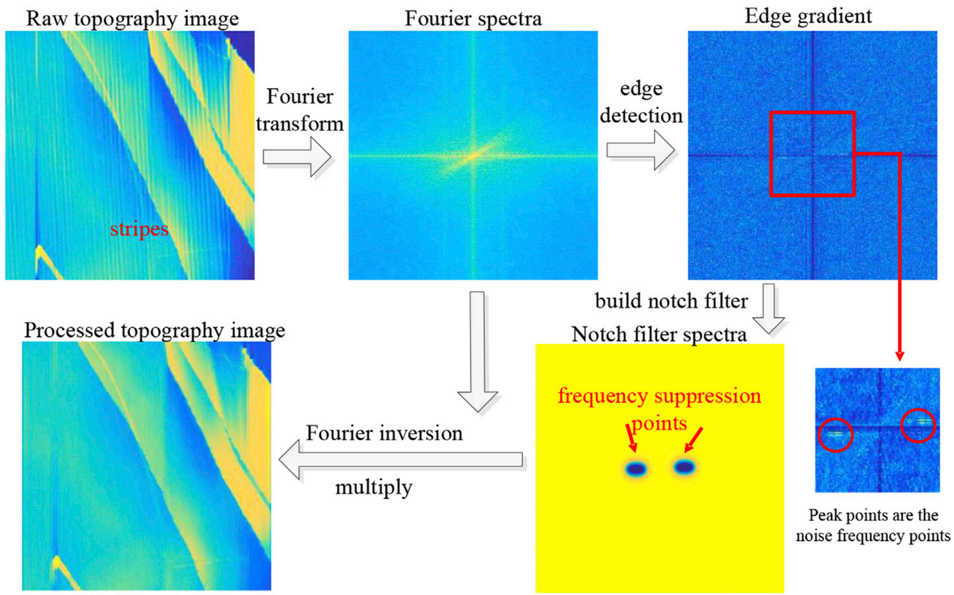

Fig. 6. Principle of the proposed method to suppress fringes. The method can be divided into four steps: 1. Fourier transform; 2. Edge detection and peak searching; 3. Notch filter; 4. Fourier inversion.

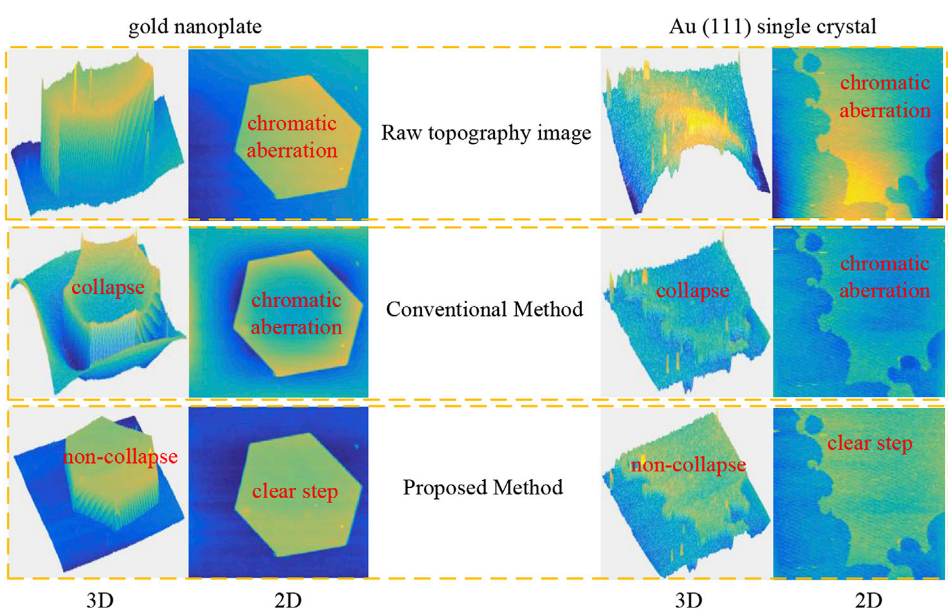

Fig. 7. Contrast between conventional method and the proposed method. The two samples were gold nanoplate and Au (111) single crystal. (For interpretation of the references to colour in this figure legend, the reader is referred to the Web version of this article.)

3.2. Image inpainting

As mentioned before, TV and Criminisi algorithms can deal with different conditions of damages. So in this part, the contrast between two algorithms was made first, as shown in Fig. 8. Both algorithms were adopted to inpaint the topography images of Au (111) single crystal with boundary damage and thiol monolayer self-assembled on Au (111) with large scale damage caused by the impurities on the surface. TV algorithm can inpaint boundary damage very well and did nothing to the large scale damage, and Criminisi algorithm obtained an undesired broken boundary and well inpainted image with large scale damage. Therefore, TV algorithm was suitable for the damages with clear boundary structural information nearby, and Criminisi algorithm was suitable for the damages with similar texture nearby. Three other damaged topography images were used to verify the algorithms, as shown in Fig. 9. The damages of them were caused by vibrating interference and response delay from control system. In particular, the last image of molybdenum disulfide had both two kinds of damages, so the two algorithms were both adopted and the inpainting worked well.

3.3. Fringe-suppression

Three topography images with clear fringes were processed, as shown in Fig. 10. The fringes of the images were suppressed significantly, but not totally eliminated. The reason was that the proposed method was a frequency domain method while the frequencies of the fringes and the

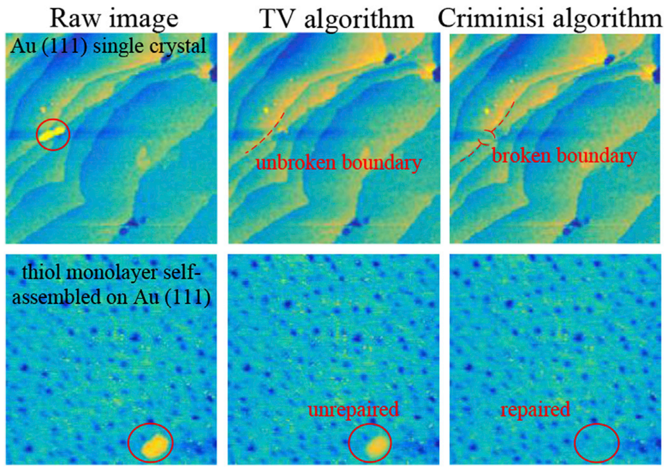

Fig. 8. Contrast between TV and Criminisi algorithms. The two samples were Au (111) single crystal and thiol monolayer self-assembled on Au (111).

sample outlines were very close or even overlapping. So the balance between them needed to be controlled artificially by adjusting the parameters of the notch filter to suppress the fringes and keep the outlines as much as possible. For example, the orders of the notch filters in Fig. 10 were all four, and the notch points were ellipse for the first two images (long axle/short axle: 30 pixels/2 pixels and 15 pixels/3 pixels) and circle for the last image (radius: 10 pixels).

4. Conclusions

We have proposed three topography image processing methods in which several algorithms are adopted according to the characteristics of the topography images. The background subtraction method uses the B-spline algorithm to better fit the background surface and the mask

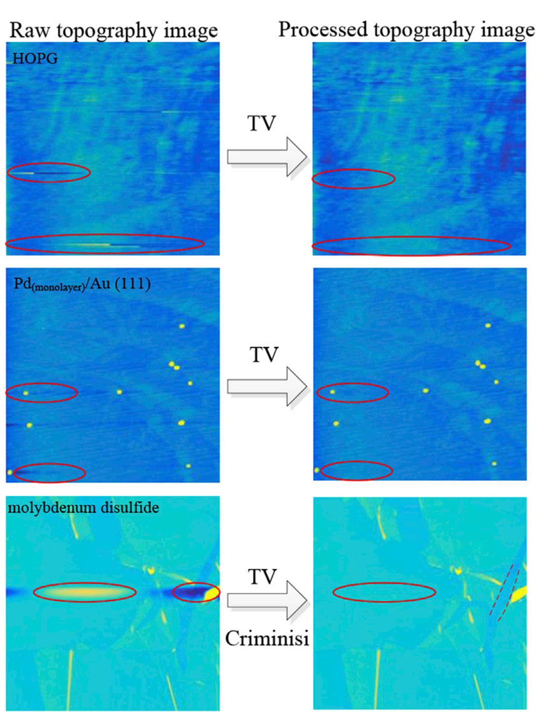

Fig. 9. Inpainting effects of the TV and Criminisi algorithms. The three samples were highly oriented pyrolytic graphite (HOPG), $Pd_{(monolayer)}$/Au (111) and molybdenum disulfide.

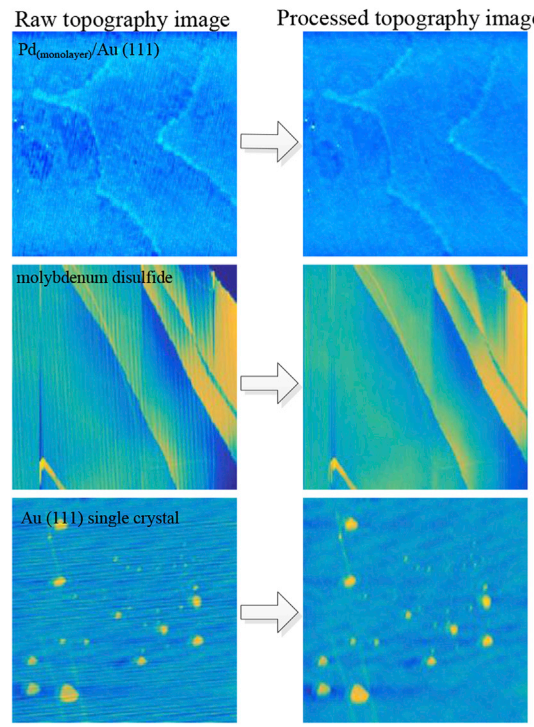

Fig. 10. Fringe-suppression effects of the proposed method. The three samples were $Pd_{(monolayer)}$/Au (111), molybdenum disulfide and Au (111) single crystal.

generator to avoid collapse and chromatic aberration in the step regions. The image inpainting method uses the TV and Criminisi algorithms to deal with the boundary damage and large scale damage respectively. The Flourier transform and notch filter are combined together to suppress the fringe caused by the periodic noise. The processing results demonstrate the effectiveness of the method adequately. The proposed methods have been written in the software, and all the methods can process one image in seconds.

Further research should be focus on the full-automatic processing. In the current software, the choice of TV and Criminisi algorithms, the damage area marking and the shape of the notch filter centers need to be decided artificially.

Notes

The authors declare no competing financial interest.

Acknowledgment

This work was supported by the National Natural Science Foundation of China (No. 21503171 & 21874113).

Appendix A. Supplementary data

Supplementary data to this article can be found online at https://doi.org/10.1016/j.chemolab.2018.12.013.

References

[1] E. Madej, N. Spiridis, R.P. Socha, B. Wolanin, Korecki, The nucleation, growth and thermal stability of iron clusters on a TiO2(110) surface, J. Appl. Surf. Sci. 416 (2017) 144–151.

[2] Y.Q. Geng, Y.D. Yan, E. Brousseau, Y.W. Sun, AFM tip-based mechanical nanomachining of 3D micro and nano-structures via the control of the scratching trajectory, J. Mater. Process. Technol. 248 (2017) 236–248.

[3] S.Y. Park, R. Elbersen, J. Huskens, H. Gardeniers, J.Y. Lee, G. Mul, J. Heo, Characterization of opto-electrical enhancement of tandem photoelectrochemical cells by using photoconductive-AFM, Nanotechnology 28 (2017), 295401.

[4] M.L. Hughes, L. Dougan, The physics of pulling polyproteins: a review of single molecule force spectroscopy using the AFM to study protein unfolding, Rep. Prog. Phys. 79 (2016), 076601.

[5] A. Noy, Force spectroscopy 101: how to design, perform, and analyze an AFM-based single molecule force spectroscopy experiment, Curr. Biol. 15 (2011) 710–718.

[6] J.H. Zhong, X. Jin, L.Y. Meng, X. Wang, H.S. Su, Z.L. Yang, C.T. Williams, B. Ren, Probing the electronic and catalytic properties of a bimetallic surface with 3 nm resolution, Nat. Nanotechnol. 12 (2017) 132–136.

[7] C. Manzano, W.H. Soe, H. Kawai, M. Saeys, C. Joachim, Origin of the apparent (2x1) topography of the Si(100)-c(4x2) surface observed in low-temperature STM images, Phys. Rev. B 83 (2011), 201302.

[8] M. Dukic, J.D. Adams, G.E. Fantner, Piezoresistive AFM cantilevers surpassing standard optical beam deflection in low noise topography imaging, Sci. Rep.-UK 5 (2015), 16393.

[9] Y.F. Zhang, B.N. Dai, Y. Deng, Y.Y. Zhao, AFM and NMR imaging of squid tropomyosin Tod p1 subjected to high hydrostatic pressure: evidence for relationships among topography, characteristic domain and allergenicity, RSC Adv. 5 (2015) 73207–73216.

[10] I. Horcas, R. Fernandez, J.M. Gomez-Rodriguez, J. Colchero, J. Gomez-Herrero, A.M. Baro, WSXM: a software for scanning probe microscopy and a tool for nanotechnology, Rev. Sci. Instrum. 78 (2007), 013705.

[11] B.W. Erickson, S. Coquoz, J.D. Adams, D.J. Burns, G.E. Fantner, Large-scale analysis of high-speed atomic force microscopy data sets using adaptive image processing, Beilstein J. Nanotechnol. 3 (2012) 747–758.

[12] H. OLIN, Design of A Scanning probe microscope, Meas. Sci. Technol. 5 (1994) 976–984.

[13] J.E. Griffith, D.A. Grigg, M.J. Vasile, P.E. Russell, E.A. Fitzgerald, Scanning probe metrology, J. Vac. Sci. Technol., A 10 (1992) 674–678.

[14] G. Renner, V. Weiß, Comput. Exact and approximate computation of B-spline curves on surfaces, Aided Design 36 (2004) 351–362.

[15] T.F. Chan, J.H. Shen, Mathematical models for local nontexture inpaintings, SIAM J. Appl. Math. 62 (2002) 1019–1043.

[16] A. Criminisi, P. Perez, K. Toyama, Object removal by exemplar-based inpainting, IEEE Proc. CVPR. 2 (2003) 721–728.

[17] J.H. Massig, J. Heppner, Fringe-pattern analysis with high accuracy by use of the Fourier-transform method: theory and experimental tests, Appl. Optic. 40 (2001) 2081–2088.